Unified Description of ^{6}Li Structure and Deuterium-^{4}He Dynamics with Chiral Two- and Three-Nucleon Forces

Guillaume Hupin,[1,*] Sofia Quaglioni,[1,†] and Petr Navrátil[2,‡]
[1]*Lawrence Livermore National Laboratory, P.O. Box 808, L-414, Livermore, California 94551, USA*
[2]*TRIUMF, 4004 Wesbrook Mall, Vancouver, British Columbia V6T 2A3, Canada*
(Received 12 December 2014; published 29 May 2015)

We provide a unified *ab initio* description of the ^{6}Li ground state and elastic scattering of deuterium (d) on ^{4}He (α) using two- and three-nucleon forces from chiral effective field theory. We analyze the influence of the three-nucleon force and reveal the role of continuum degrees of freedom in shaping the low-lying spectrum of ^{6}Li. The calculation reproduces the empirical binding energy of ^{6}Li, yielding an asymptotic D- to S-state ratio of the ^{6}Li wave function in the $d+\alpha$ configuration of -0.027, in agreement with a determination from ^{6}Li-^{4}He elastic scattering, but overestimates the excitation energy of the 3^+ state by 350 keV. The bulk of the computed differential cross section is in good agreement with data. These results endorse the application of the present approach to the evaluation of the $^2\mathrm{H}(\alpha,\gamma)^6\mathrm{Li}$ radiative capture, responsible for the big-bang nucleosynthesis of ^{6}Li.

DOI: 10.1103/PhysRevLett.114.212502 PACS numbers: 21.60.De, 24.10.Cn, 25.45.-z, 27.20.+n

Introduction.—Lithium-6 (^{6}Li) is a weakly bound stable nucleus that breaks into an ^{4}He (or α particle) and a deuteron (d) at the excitation energy of 1.4743 MeV [1]. A complete unified treatment of the bound and continuum properties of this system is desirable to further our understanding of the fundamental interactions among nucleons, but also to inform the evaluation of low-energy cross sections relevant to applications. Notable examples are the $^2\mathrm{H}(\alpha,\gamma)^6\mathrm{Li}$ radiative capture (responsible for the big-bang nucleosynthesis of ^{6}Li [2–6]) and the $^2\mathrm{H}(\alpha,d)^4\mathrm{He}$ cross section used in the characterization of deuteron concentrations in thin films [7–9]. Contrary to the lighter nuclei, the structure of the ^{6}Li ground state (g.s.)—namely, the amount of the D-state component in its $d+\alpha$ configuration—is still uncertain [1]. Well known experimentally, the low-lying resonances of ^{6}Li have been shown to present significant sensitivity to three-nucleon ($3N$) interactions in *ab initio* calculations that treated them as bound states [10–13]. However, this approximation is well justified only for the narrow 3^+ first excited state, and no information about the widths was provided. At the same time, the only *ab initio* study of d-^{4}He scattering [14] was based on a nucleon-nucleon (NN) Hamiltonian and did not take into account the swelling of the α particle due to the interaction with the deuteron.

As demonstrated in a study of the unbound ^{7}He nucleus, the *ab initio* no-core shell model with continuum (NCSMC) [15] is an efficient many-body approach to nuclear bound and scattering states alike. Initially developed to compute nucleon-nucleus collisions starting from a two-body Hamiltonian, this technique was later extended to include $3N$ forces and successfully applied to make predictions of elastic scattering and recoil of protons off ^{4}He [16] and to study continuum and $3N$-force effects on the energy levels of ^{9}Be [17]. Recently, we have developed the NCSMC formalism to describe more challenging deuterium-nucleus collisions and we present in this Letter a study of the ^{6}Li ground state and d-^{4}He elastic scattering using $NN+3N$ forces from chiral effective field theory [18,19].

Approach.—We cast the microscopic ansatz for the ^{6}Li wave function in the form of a generalized cluster expansion,

$$|\Psi^{J^\pi T}\rangle = \sum_\lambda c_\lambda |^6\mathrm{Li}\,\lambda J^\pi T\rangle + \sum_\nu \int dr r^2 \frac{\gamma_\nu(r)}{r}\mathcal{A}_\nu |\Phi^{J^\pi T}_{\nu r}\rangle, \quad (1)$$

where J, π, and T are, respectively, total angular momentum, parity, and isospin, $|^6\mathrm{Li}\,\lambda J^\pi T\rangle$ represent square-integrable energy eigenstates of the ^{6}Li system, and

$$|\Phi^{J^\pi T}_{\nu r}\rangle = [(|^4\mathrm{He}\,\lambda_\alpha J^{\pi_\alpha}_\alpha T_\alpha\rangle |^2\mathrm{H}\,\lambda_d J^{\pi_d}_d T_d\rangle)^{(sT)} Y_\ell(\hat{r}_{\alpha,d})]^{(J^\pi T)} \times \frac{\delta(r-r_{\alpha,d})}{r r_{\alpha,d}} \quad (2)$$

are continuous basis states built from a ^{4}He and a ^{2}H nuclei whose centers of mass are separated by the relative coordinate $\vec{r}_{\alpha,d}$, and that are moving in a $^{2s+1}\ell_J$ partial wave of relative motion. The translationally invariant compound, target, and projectile states (with energy labels λ, λ_α, and λ_d, respectively) are all obtained by means of the no-core shell model (NCSM) [20,21] using a basis of many-body harmonic oscillator (HO) wave functions with frequency $\hbar\Omega$ and up to $N_{\max}$ HO quanta above the lowest

energy configuration. The index ν collects the quantum numbers $\{^4\mathrm{He}\,\lambda_\alpha J^{\pi_\alpha}_\alpha T_\alpha; {}^2\mathrm{H}\,\lambda_d J^{\pi_d}_d T_d; s\ell\}$ associated with the continuous basis states of Eq. (2), and the operator (with $P_{i,j}$ exchanging particles i and j),

$$\mathcal{A}_\nu = \frac{1}{\sqrt{15}}\left(1 - \sum_{i=1}^{4}\sum_{j=5}^{6} P_{i,j} + \sum_{i<j=1}^{4} P_{i,5}P_{j,6}\right),$$

ensures its full antisymmetrization. Expansion (1) is further orthonormalized to account for the overcompleteness of the basis [15]. Finally, the unknown discrete coefficients c_λ and continuous amplitudes of relative motion $\gamma_\nu(r)$ are obtained by solving the six-body Schrödinger equation in the Hilbert space spanned by the basis states $|^6\mathrm{Li}\,\lambda J^\pi T\rangle$ and $\mathcal{A}_\nu|\Phi^{J^\pi T}_{\nu r}\rangle$ [15]. The bound state and the elements of the scattering matrix are then obtained from matching the orthogonalized expansion (1) with the known asymptotic behavior of the wave function using an extension of the microscopic R-matrix theory [22,23].

The deuteron is only bound by 2.224 MeV. For relative kinetic energies (E_{kin}) above this threshold, the d-^{4}He scattering problem is of a three-body nature (until the breakup of the tightly bound ^{4}He, that is). Below, the virtual scattering to the energetically closed $^4\mathrm{He} + p + n$ channels accounts for the distortion of the projectile. Here we address this by discretizing the continuum of ^{2}H in the $^3S_1 - {}^3D_1$, $^3D_2$, and $^3D_3 - {}^3G_3$ channels identified in our earlier study of Ref. [14]. At the same time, the first fifteen (all energetically relevant positive- and negative-parity states up to $J = 3$) square-integrable six-body eigenstates of ^{6}Li also contribute to the description of the deuteron distortion. More importantly, they address the swelling of the α particle, of which we can (computationally) afford to include only the g.s. This was demonstrated in Ref. [16], where proton-^{4}He scattering phase shifts were shown to be rather insensitive to the inclusion of ^{4}He excitations, once ^{5}Li square-integrable states were added to the description. The typical convergence behavior of our computed d-^{4}He phase shifts with respect to the number of deuteron pseudostates (or $d^\star$, with $E_{d^\star} > 0$) included in Eq. (2) is shown in Fig. 1. Stable results are found with as little as three pseudostates per channel, less than half than in the more limited study of Ref. [14], lacking the coupling of square-integrable ^{6}Li eigenstates. Nonetheless, above the ^{2}H breakup threshold, our approach is approximated and a rigorous treatment would require the more complicated task of including three-cluster basis states [24] in the ansatz of Eq. (1).

The treatment of $3N$ forces within the NCSMC formalism to compute deuteron-nucleus collisions involves major technical and computational challenges. The first is the derivation and calculation of the matrix elements between the continuous basis states of Eq. (2) of seven

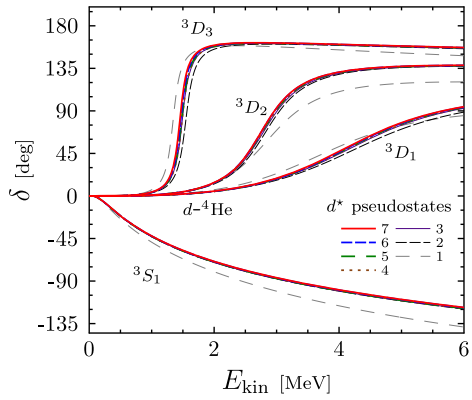

FIG. 1 (color online). Computed d-^{4}He S- and D-wave phase shifts at $N_{\max} = 8$ and $\hbar\Omega = 20$ MeV, obtained with fifteen square-integrable ^{6}Li eigenstates and up to seven ^{2}H pseudostates in each of the $^3S_1 - {}^3D_1$, $^3D_2$, and $^3D_3 - {}^3G_3$ channels. The two-body part of the similarity renormalization group (SRG) evolved N^{3}LO NN potential [25] (NN-only) with $\Lambda = 2.0$ fm^{-1} was used.

independent $3N$-force terms, five of which involve operations on three to four nucleons of the target, e.g., $\langle\Phi^{J^\pi T}_{\nu' r'}|P_{3,5}P_{4,6}V^{3N}_{123}|\Phi^{J^\pi T}_{\nu r}\rangle$, with V^{3N}_{123} the $3N$ interaction among particles 1,2, and 3. To calculate these contributions, we need the three- and four-nucleon densities of the target [26]. An additional difficulty is represented by the exorbitant number of input $3N$-force matrix elements (see Fig. 1 of Ref. [27]), which we include up to a maximum three-nucleon HO model space of seventeen major shells. The $\langle{}^6\mathrm{Li}\,\lambda J^\pi T|V^{3N}_{346}|\Phi^{J^\pi T}_{\nu r}\rangle$ and $\langle{}^6\mathrm{Li}\,\lambda J^\pi T|V^{3N}_{456}|\Phi^{J^\pi T}_{\nu r}\rangle$ couplings between discrete and continuous states are comparatively less demanding.

Results.—We adopt a Hamiltonian based on the chiral N^{3}LO NN interaction of Ref. [25] and the N^{2}LO $3N$ force of Ref. [28], constrained to provide an accurate description

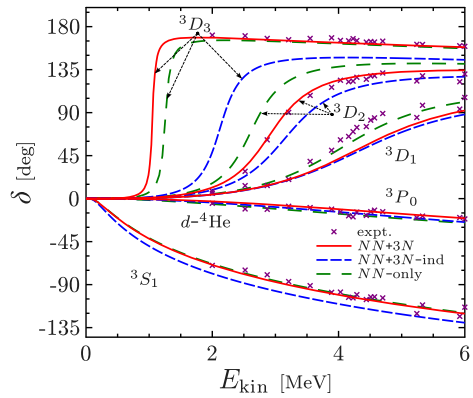

FIG. 2 (color online). S-, $^3P_0$-, and D-wave d-^{4}He phase shifts computed with the NN-only, $NN + 3N$-ind, and $NN + 3N$ Hamiltonians (lines) compared to those of the R-matrix analyses of [34,35] (symbols). More details in the text.

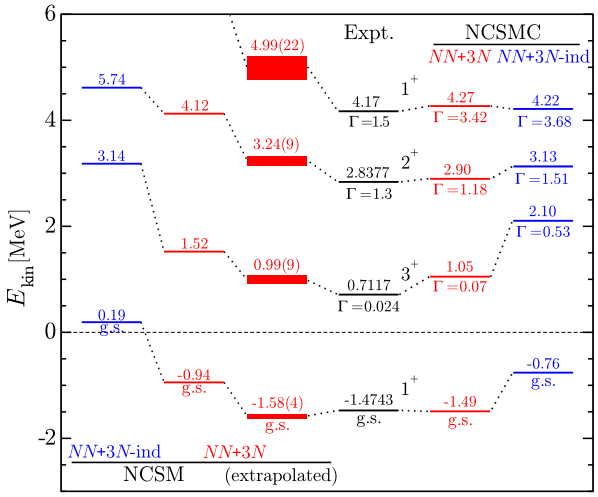

FIG. 3 (color online). Ground-state energy and low-lying ^{6}Li positive-parity $T = 0$ resonance parameters extracted [36] from the phase shifts of Fig. 2 (NCSMC) compared to the evaluated centroids and widths (indicated by Γ) of Ref. [1] (Expt.). Also shown on the left-hand side are the best ($N_{\max} = 12$) and extrapolated [37] NCSM energy levels. The zero energy is set to the respective computed (experimental) $d + {}^4$He breakup thresholds. Absolute g.s. energies can be found in Table I.

of the $A = 2$ and 3 [29] systems. These interactions are additionally softened by means of a unitary transformation that decouples high- and low-momentum components, working within the similarity renormalization group (SRG) method [27,30–33]. To minimize the occurrence of induced four-nucleon forces, we work with the SRG resolution scale $\Lambda = 2.0$ fm^{-1} [26,32,33]. All calculations are carried out, including the first fifteen $J^\pi \leq 3^\pm$ (of which two 1^+ and 2^+, and one 3^+) discrete eigenstates of the ^{6}Li system and continuous d-^{4}He(g.s.) states with up to seven deuteron pseudostates in the $^3S_1 - {}^3D_1$, $^3D_2$, and $^3D_3 - {}^3G_3$ channels. Similar to our earlier study performed with a softer NN interaction but in a model space spanned only by the continuous basis states of Eq. (2) [14], we approach convergence for the HO expansions at $N_{\max} = 10(11)$ for positive (negative) parity channels. We adopt the HO frequency of 20 MeV around which the ^{6}Li g.s. energy calculated within the square-integrable basis of the NCSM becomes nearly insensitive to $\hbar\Omega$ [13].

In Fig. 2, we compare our computed d-^{4}He S-, $^3P_0$-, and D-wave phase shifts with those of the R-matrix analyses of Refs. [34,35]. The results based on the two-body part of the SRG-transformed NN force (NN-only) resemble those of Ref. [14]. Once the SRG unitary equivalence is restored via the induced $3N$ force ($NN + 3N$-ind), the resonance centroids are systematically shifted to higher energies. By contrast, the agreement with data is much improved when the initial chiral $3N$ force is also included ($NN + 3N$). In particular, the splitting between the $^3D_3$ and $^3D_2$ partial waves is comparable to experiment.

In Fig. 3, the resonance centroids and widths extracted [36] from the phase shifts of Fig. 2 (shown on the right) are compared with experiment as well as with more traditional approximated energy levels (shown on the left) obtained within the NCSM by treating the ^{6}Li excited states as bound states. In terms of excitation energies relative to the g.s., in both calculations (i.e., with or without continuum effects) the chiral $3N$ force affects mainly the splitting between the 3^+ and 2^+ states, and to a lesser extent the position of the first excited state. Sensitivity to the chiral $3N$ force is also seen in the widths of the NCSMC resonances, which tend to become narrower (in closer agreement with experiment) when this force is present in the initial Hamiltonian. Overall, the closest agreement with the observed spectrum is obtained with the $NN + 3N$ Hamiltonian working within the NCSMC, i.e., by including the continuum degrees of freedom. Incidentally, we note that the NN-only Hamiltonian (not shown in Fig. 3) yields g.s. and 3^+ energies (with respect to the computed $d + {}^4$He threshold) close to the $NN + 3N$ results, e.g. -1.62 and 1.24 MeV, respectively, within the NCSMC. However, the splitting between 2^+ and 3^+ is smaller. Compared to the best ($N_{\max} = 12$) NCSM values, all resonances are shifted to lower energies commensurately with their distance from the breakup threshold. For the 3^+, which is a narrow resonance, the effect is not sufficient to correct for the slight overestimation in excitation energy already observed in the NCSM calculation. This and the ensuing underestimation of the splitting between the 2^+ and 3^+ states point to remaining deficiencies in the

TABLE I. Absolute ^{6}Li g.s. energy, S- (C_0) and D-wave (C_2) asymptotic normalization constants and their ratio using the $NN + 3N$ Hamiltonian compared to experiment. Also shown is the sum of ^{4}He and ^{2}H g.s. energies, $E_\alpha + E_d$. Indicated in parenthesis is the $N_{\max}$ value of the respective calculation.

Ground-state properties	NCSM (10)	NCSM (12)	NCSM (∞) [37]	NCSMC (10)	Experiment		
$E_{^6\mathrm{Li}}$ [MeV]	−30.84	−31.52	−32.19(1)	−32.01	−31.994 [1,40]		
C_0 [fm$^{-1/2}$]				2.695	2.91(9) [39]	2.93(15)	[41]
C_2 [fm$^{-1/2}$]				−0.074	−0.077(18) [39]		
C_2/C_0				−0.027	−0.025(6)(10) [39]	0.0003(9)	[38]
$E_\alpha + E_d$ [MeV]	−30.52	−30.58	−30.61(4)	−30.52	−30.520		

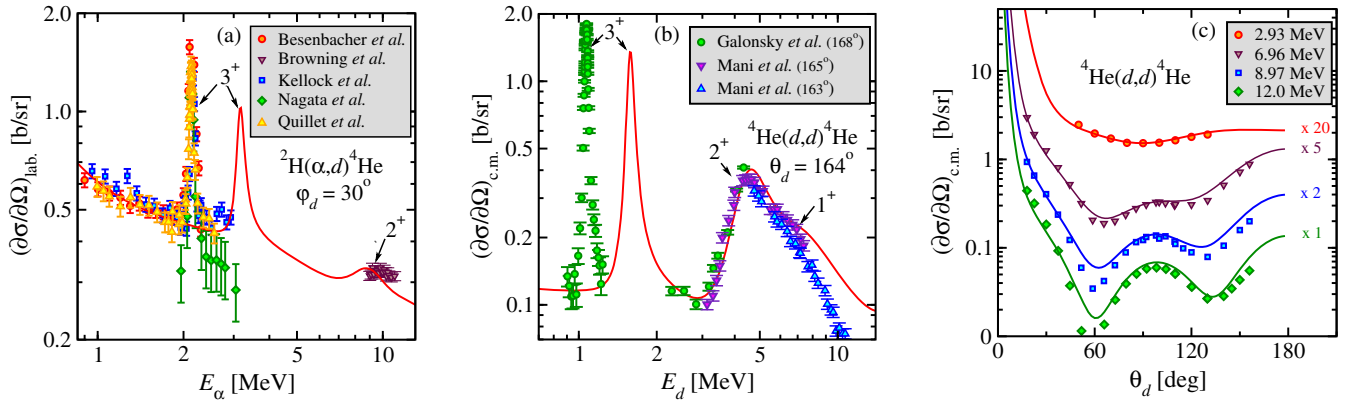

FIG. 4 (color online). Computed (a) $^2\mathrm{H}(\alpha, d)^4\mathrm{He}$ laboratory-frame and (b) $^4\mathrm{He}(d, d)^4\mathrm{He}$ center-of-mass frame angular differential cross sections (lines) using the $NN + 3N$ Hamiltonian at the deuteron laboratory and c.m. angles of, respectively, $\varphi_d = 30°$ and $\theta_d = 164°$ as a function of the laboratory helium (E_α) and deuteron (E_d) incident energies, compared with data (symbols) from Refs. [7–9,42–45]. (c) Calculated (lines) and measured (symbols) center-of-mass angular distributions at $E_d = 2.93, 6.96, 8.97$ [46], and 12 MeV [47] are scaled by a factor of 20,5,2, and 1, respectively. All positive- and negative-parity partial waves up to $J = 3$ were included in the calculations.

adopted $3N$ force model, particularly concerning the strength of the spin-orbit interaction.

The inclusion of the $d + {}^4\mathrm{He}$ states of Eq. (2) results also in additional binding for the 1^+ ground state. This stems from a more efficient description of the clusterization of ^{6}Li into $d + \alpha$ at long distances, which is harder to describe within a finite HO model space, or—more simply—from the increased size of the many-body model space. Indeed, as shown in Fig. 3 and in Table I for the absolute value of the ^{6}Li g.s. energy, extrapolating to $N_{\max} \to \infty$ [37] brings the NCSM results into good agreement with the NCSMC, for bound states and narrow resonances. However, only with the latter do the wave functions present the correct asymptotic, which for the g.s. are Whittaker functions. This is essential for the extraction of the asymptotic normalization constants and a future description of the $^2\mathrm{H}(\alpha, \gamma)^6\mathrm{Li}$ radiative capture [5]. The obtained asymptotic D- to S-state ratio is not compatible with the near-zero value of Ref. [38], but rather is in good agreement with the determination of Ref. [39], stemming from an analysis of $^6\mathrm{Li} + {}^4\mathrm{He}$ elastic scattering.

Next, in Figs. 4(a) and 4(b), respectively, we compare the $^2\mathrm{H}(\alpha, d)^4\mathrm{He}$ deuteron elastic recoil and $^4\mathrm{He}(d, d)^4\mathrm{He}$ deuteron elastic scattering differential cross sections computed using the $NN + 3N$ Hamiltonian to the measured energy distributions of Refs. [7–9,42–45]. Aside from the position of the 3^+ resonance, the calculations are in fair agreement with experiment, particularly in the low-energy region of interest for the big-bang nucleosynthesis of ^{6}Li, where we reproduce the data of Besenbacher *et al.* [42] and Quillet *et al.* [8]. The 500 keV region below the resonance in Fig. 4(a) is also important for material science, where the elastic recoil of deuterium knocked by incident α particles is used to analyze the presence of ^{2}H. At higher energies, near the 2^+ and 1^+ resonances, the computed cross section at the center-of-mass scattering angle of $\theta_d = 164°$ reproduces the data of Galonsky *et al.* [44] and Mani *et al.* [45], while we find slight disagreement with the data of Ref. [9] in the elastic recoil configuration at the laboratory angle of $\varphi_d = 30°$. At even higher energies, the calculated cross section of Fig. 4(b) lies above the measured one. This is likely related to the fact that the 1^+_2 state is too broad. The overall good agreement with experiment is also corroborated by Fig. 4(c), presenting $^4\mathrm{He}(d, d)^4\mathrm{He}$ angular distributions in the $2.93 \le E_d \le 12.0$ MeV interval of incident energies. In particular, the theoretical curves reproduce the data at 2.93 and 6.96 MeV, while some deviations are visible at the two higher energies, in line with our previous discussion. Nevertheless, in general, the present results with $3N$ forces provide a much more realistic description of the scattering process than our earlier study of Ref. [14]. Finally, we expect that an $N_{\max} = 12(13)$ calculation (currently out of reach) would not significantly change the present picture, particularly concerning the narrow 3^+ resonance. Indeed, much as in the case of the g.s. energy, here the NCSMC centroid is in good agreement with the NCSM extrapolated value, 0.99(9) MeV.

Conclusions.—We presented an application of the *ab initio* NCSMC formalism to the description of deuteron-nucleus dynamics. We illustrated the role of the chiral $3N$ force and continuous degrees of freedom in determining the bound-state properties of ^{6}Li and d-^{4}He elastic scattering observables. The computed g.s. energy is in excellent agreement with experiment, and our $d + \alpha$ asymptotic normalization constants support a nonzero negative ratio of D- to S-state components for ^{6}Li. We used deuterium backscattering and recoil cross-section data of interest to ion beam spectroscopy to validate our scattering calculations and found good agreement at low energy in particular. The overestimation by about 350 keV of the position of the 3^+ resonance is an indication of remaining deficiencies of the Hamiltonian

employed here. This work sets the stage for an *ab initio* study of the ^{2}H$(\alpha,\gamma)^6$Li radiative capture, and is a stepping stone in the calculation of the deuterium-tritium fusion with the chiral $NN+3N$ Hamiltonian, currently in progress.

Computing support for this work came from the Lawrence Livermore National Laboratory (LLNL) institutional Computing Grand Challenge program. This work was prepared in part by LLNL under Contract No. DE-AC52-07NA27344. This material is based upon work supported by the U.S. Department of Energy, Office of Science, Office of Nuclear Physics, under Work Proposal No. SCW1158, and by the NSERC Grant No. 401945-2011. TRIUMF receives funding via a contribution through the Canadian National Research Council.

*hupin@ipnorsay.in2p3.fr
Present address: Institut de Physique Nucléaire, IN2P3-CNRS, Université Paris-Sud, F-91406 Orsay Cedex, France.
†quaglioni1@llnl.gov
‡navratil@triumf.ca

[1] D. R. Tilley, C. M. Cheves, J. L. Godwin, G. M. Hale, H. M. Hofmann, J. H. Kelley, C. G. Sheu, and H. R. Weller, Nucl. Phys. **A708**, 3 (2002).
[2] K. M. Nollett, M. Lemoine, and D. N. Schramm, Phys. Rev. C **56**, 1144 (1997).
[3] K. M. Nollett, R. B. Wiringa, and R. Schiavilla, Phys. Rev. C **63**, 024003 (2001).
[4] F. Hammache *et al.*, Phys. Rev. C **82**, 065803 (2010).
[5] A. M. Mukhamedzhanov, L. D. Blokhintsev, and B. F. Irgaziev, Phys. Rev. C **83**, 055805 (2011).
[6] M. Anders *et al.*, Phys. Rev. Lett. **113**, 042501 (2014).
[7] A. J. Kellock and J. E. E. Baglin, Nucl. Instrum. Methods Phys. Res., Sect. B **79**, 493 (1993).
[8] V. Quillet, F. Abel, and M. Schott, Nucl. Instrum. Methods Phys. Res., Sect. B **83**, 47 (1993).
[9] J. F. Browning, J. C. Banks, W. R. Wampler, and B. L. Doyle, Nucl. Instrum. Methods Phys. Res., Sect. B **219–220**, 317 (2004).
[10] S. C. Pieper, V. R. Pandharipande, R. B. Wiringa, and J. Carlson, Phys. Rev. C **64**, 014001 (2001).
[11] P. Navrátil and W. E. Ormand, Phys. Rev. C **68**, 034305 (2003).
[12] S. C. Pieper, R. B. Wiringa, and J. Carlson, Phys. Rev. C **70**, 054325 (2004).
[13] E. D. Jurgenson, P. Navrátil, and R. J. Furnstahl, Phys. Rev. C **83**, 034301 (2011).
[14] P. Navrátil and S. Quaglioni, Phys. Rev. C **83**, 044609 (2011).
[15] S. Baroni, P. Navrátil, and S. Quaglioni, Phys. Rev. Lett. **110**, 022505 (2013); Phys. Rev. C **87**, 034326 (2013).
[16] G. Hupin, S. Quaglioni, and P. Navrátil, Phys. Rev. C **90**, 061601 (2014).
[17] J. Langhammer, P. Navrátil, S. Quaglioni, G. Hupin, A. Calci, and R. Roth, Phys. Rev. C **91**, 021301 (2015).
[18] E. Epelbaum, H.-W. Hammer, and U.-G. Meißner, Rev. Mod. Phys. **81**, 1773 (2009).
[19] R. Machleidt and D. R. Entem, Phys. Rep. **503**, 1 (2011).
[20] P. Navrátil, J. P. Vary, and B. R. Barrett, Phys. Rev. Lett. **84**, 5728 (2000).
[21] B. R. Barrett, P. Navrátil, and J. P. Vary, Prog. Part. Nucl. Phys. **69**, 131 (2013).
[22] M. Hesse, J.-M. Sparenberg, F. Van Raemdonck, and D. Baye, Nucl. Phys. **A640**, 37 (1998).
[23] M. Hesse, J. Roland, and D. Baye, Nucl. Phys. **A709**, 184 (2002).
[24] C. Romero-Redondo, S. Quaglioni, P. Navrátil, and G. Hupin, Phys. Rev. Lett. **113**, 032503 (2014).
[25] D. R. Entem and R. Machleidt, Phys. Rev. C **68**, 041001 (2003).
[26] G. Hupin, J. Langhammer, P. Navrátil, S. Quaglioni, A. Calci, and R. Roth, Phys. Rev. C **88**, 054622 (2013).
[27] R. Roth, A. Calci, J. Langhammer, and S. Binder, Phys. Rev. C **90**, 024325 (2014).
[28] P. Navrátil, Few-Body Syst. **41**, 117 (2007).
[29] D. Gazit, S. Quaglioni, and P. Navrátil, Phys. Rev. Lett. **103**, 102502 (2009).
[30] S. K. Bogner, R. J. Furnstahl, and R. J. Perry, Phys. Rev. C **75**, 061001 (2007).
[31] H. Hergert and R. Roth, Phys. Rev. C **75**, 051001 (2007).
[32] E. D. Jurgenson, P. Navrátil, and R. J. Furnstahl, Phys. Rev. Lett. **103**, 082501 (2009).
[33] R. Roth, J. Langhammer, A. Calci, S. Binder, and P. Navrátil, Phys. Rev. Lett. **107**, 072501 (2011).
[34] W. Grüebler, P. A. Schmelzbach, V. König, R. Risler, and D. Boerma, Nucl. Phys. **A242**, 265 (1975).
[35] B. Jenny, W. Grüebler, V. König, P. A. Schmelzbach, and C. Schweizer, Nucl. Phys. **A397**, 61 (1983).
[36] Centroids E_R and widths Γ are obtained, respectively, as the values of $E_{\rm kin}$ for which the first derivative $\delta'(E_{\rm kin})$ of the phase shifts is maximal and $\Gamma = 2/\delta'(E_R)$.
[37] Extrapolated values E_∞ are obtained from fitting the $N_{\rm max} = 6$ to 12 energies at $\hbar\Omega = 20$ MeV with the function $E(N_{\rm max}) = E_\infty + a\exp(-bN_{\rm max})$.
[38] K. D. Veal, C. R. Brune, W. H. Geist, H. J. Karwowski, E. J. Ludwig, A. J. Mendez, E. E. Bartosz, P. D. Cathers, T. L. Drummer, K. W. Kemper, A. M. Eiró, F. D. Santos, B. Kozlowska, H. J. Maier, and I. J. Thompson, Phys. Rev. Lett. **81**, 1187 (1998).
[39] E. A. George and L. D. Knutson, Phys. Rev. C **59**, 598 (1999).
[40] G. Audi, F. G. Kondev, M. Wang, B. Pfeiffer, X. Sun, J. Blachot, and M. MacCormick, Chin. Phys. C **36**, 1157 (2012).
[41] L. D. Blokhintsev, V. I. Kukulin, A. A. Sakharuk, D. A. Savin, and E. V. Kuznetsova, Phys. Rev. C **48**, 2390 (1993).
[42] F. Besenbacher, I. Stensgaard, and P. Vase, Nucl. Instrum. Methods Phys. Res., Sect. B **15**, 459 (1986).
[43] S. Nagata, S. Yamaguchi, Y. Fujino, Y. Hori, N. Sugiyama, and K. Kamada, Nucl. Instrum. Methods Phys. Res., Sect. B **6**, 533 (1985).
[44] A. Galonsky, R. A. Douglas, W. Haeberli, M. T. McEllistrem, and H. T. Richards, Phys. Rev. **98**, 586 (1955).
[45] G. S. Mani and A. Tarratts, Nucl. Phys. **A107**, 624 (1968).
[46] J. H. Jett, J. L. Detch, and N. Jarmie, Phys. Rev. C **3**, 1769 (1971).
[47] L. S. Senhouse and T. A. Tombrello, Nucl. Phys. **57**, 624 (1964).